Phase Behavior and Macroscopic Processing of Single-Walled Carbon Nanotube – Lysozyme Dispersions

D. W. Horn and V. A. Davis

Auburn University, Auburn, AL, USA, davisva@auburn.edu

ABSTRACT

The structural and enzymatic nature of lysozyme (LSZ) makes possible the dispersion of single-walled carbon nanotubes (SWNT) for processing into macroscopic assemblies. Increasing the concentration of uncentrifuged dispersions of LSZ-SWNT results in a phase transition from an isotropic liquid to a dispersion that behaves as a rheological gel but contains large SWNT aggregates. In contrast, supernatants from centrifuged dispersions of LSZ-SWNT does not result in the same aggregation or gelation behaviors. The previously demonstrated ability to produce aligned antibacterial LSZ-SWNT films has been extended to solution spinning of more concentrated dispersions.

1 BACKGROUND

Since 2000, communicable illnesses have cost the United States approximately $304 billion and 111 million lost work days annually.[1] Coupling LSZ's antibacterial activity with the strength and conductivity of SWNT has the potential to enable robust, multifunctional, antibacterial coatings, films, and fibers.[2]

SWNT have exceptional structural, thermal, and electrical properties, which have been widely studied since their discovery in 1991. SWNT have an average experimental Young's modulus of 1.25 TPa and an average experimental tensile strength of 37 GPa; when normalized for density these properties are approximately 20 and 60 times that of steel, respectively.[3,4] In addition, SWNT have an experimental thermal conductivity of approximately 2,300 W/m-K and an average electrical resistivity of 100 μΩ-cm.[5] Exploiting these properties requires separating the large entangled SWNT aggregates produced by most production schemes and reassembling the SWNT into larger structures with controlled microstructures. These properties can be exploited when SWNT are dispersed as individuals or small bundles.

Aqueous solutions of LSZ, a model protein discovered in 1909, have been demonstrated to be an effective dispersant of low concentrations of individual SWNT due to the LSZ's polyampholitic character and the interactions between LSZ's tryptophan residue and SWNT.[6] However, there have been no studies on the phase behavior of higher concentration dispersions in which the antibacterial activity of LSZ is maintained. The antibacterial activity of LSZ is due to its ability to catalyze the hydrolysis of the 1,4-β-glycosidic linkage between N-acetyl glucosamine and N-acetyl muramic acid found in the peptidoglycan layer of Gram-positive bacteria.[7] The disulfide bridges present in LSZ are critical to its robust thermal and structural stability; LSZ's denaturation temperature is 76^{o}C.[8]

2 DISPERSION CHARACTERIZATION

Dispersions of SWNT (SWeNT CG200, Norman, OK) and LSZ (Sigma Aldrich, St.Louis, MO) were prepared using tip sonication of aqueous SWNT-LSZ solutions. The sonication waves temporarily overcome the 500 ev/μm van der Waals force of attraction between SWNT allowing LSZ to intercalate and stabilize SWNT as individuals and bundles. Since higher concentrations are desirable for processing into films and fibers, two sample preparation methods were investigated. First, the initial dispersions

containing a mixture of individual SWNT and small aggregates were concentrated through evaporation. Second, centrifugation of LSZ-SWNT dispersions was used to remove excess SWNT and LSZ, leaving a supernatant of individual SWNT. The supernatants had a much lower initial concentration of SWNT than the bulk dispersions, but were concentrated by evaporation.

Ultraviolet-visible spectroscopy was performed on the supernatant of a 0.5 wt.% LSZ – 0.1 wt.% SWNT dispersion. Figure 1 shows the supernatant absorbance as a function of wave energy. The sharp van Hove singularities at 1.6 and 2.4 eV support the presence of individual or small bundles of SWNT and are consistent with previous work using purified HiPCO SWNT which showed the supernatants contained individually dispersed SWNT based on UV-vis of the dispersions, and both AFM and ellipsometry of dried films.[2]

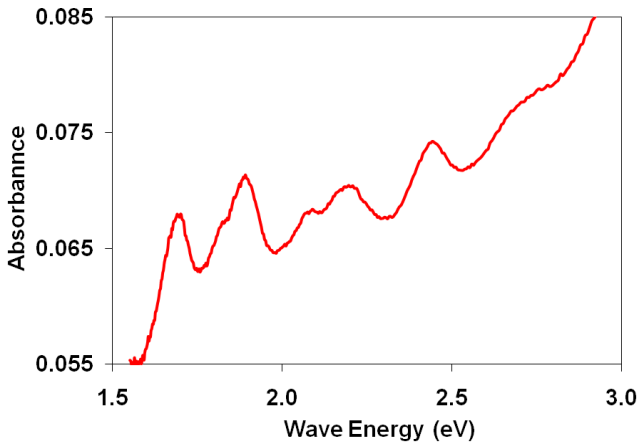

Figure 1. Ultraviolet-visible spectroscopy of the supernatant of a 0.5 wt.% LSZ – 0.1 wt.% SWNT dispersion.

Figure 2 shows scanning electron micrographs on the same dispersion. The numbered images, show an approximately 10 nm SWNT bundle coated by LSZ. The SEM images also show the close interaction between the SWNT and LSZ. In addition to using SEM to obtain microstructural detail for dried dispersions, optical microscopy was used to observe larger structures and the presence or absence of birefringence.

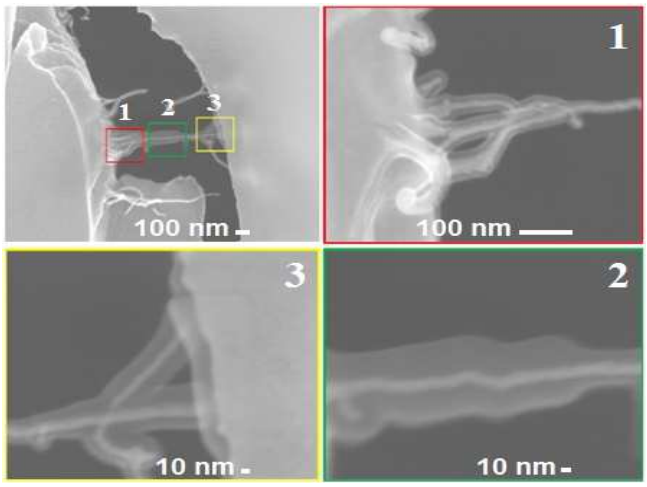

Figure 2. Scanning electron micrographs of the supernatant of a 0.5 wt.% LSZ – 0.1 wt.% SWNT dispersion.

For the initial mixtures, the weight ratio of LSZ:SWNT was varied from 10:1 to 2.5:1. The initial mixtures were then concentrated by evaporation. Figure 3 shows the phase diagram for LSZ-SWNT mixtures. For all ratios, aggregates are present from the outset. However, for all cases there was an observable change in the size of aggregates. The critical SWNT concentration at which the change occurred was 0.1 vol.% for all ratios. This transition, indicated by a red line in Figure 3, corresponded to a change in the rheological properties of the dispersions. Figure 4 shows that the slope of G', the elastic modulus, changes with increasing concentration. At 0.406 and 0.601 vol.% SWNT, G' is virtually constant throughout the entire frequency range. This is indicative of the formation of a network or gel. The transition concentrations for each LSZ:SWNT ratio can be quantitatively compared using the phase angle $\tan(\delta) = G''/G'$ as shown in Table 1. The onset of large aggregates at the same concentration where there is an abrupt change in $\tan(\delta)$ suggests that gelation and aggregation are connected. It is hypothesized that at the transition concentration the SWNT aggregate due to a depletion type interaction. This reduces the amount of LSZ that is closely associated with SWNT and increases the concentration of free LSZ resulting in a sufficiently high concentration for LSZ gel

formation. The optical phase transition is seen as the point at which aggregation occurs due to the depletion interaction between LSZ and SWNT.

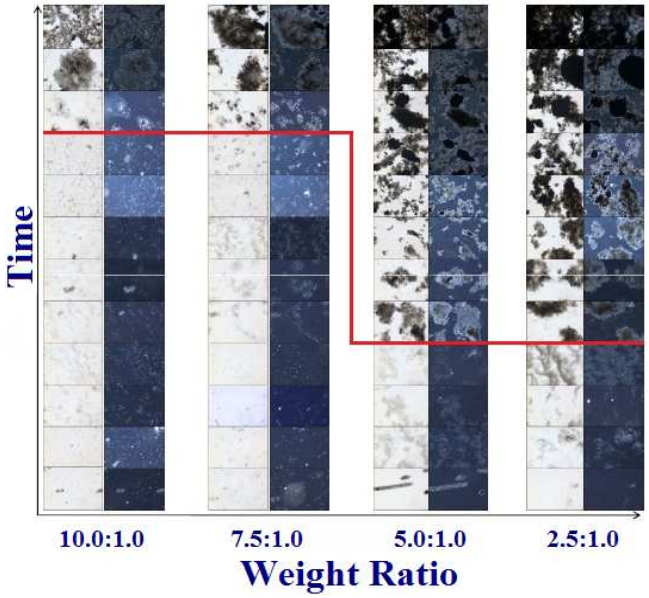

Figure 3. Phase diagram of LSZ-SWNT mixture dispersions showing concentration as a function of LSZ:SWNT weight ratios.

3 MACROSCOPIC ASSEMBLY

Initial progress was made on fiber spinning and film casting concentrated LSZ-SWNT mixtures. As previously observed for both solution spun polymer fibers and carbon nanotube fibers, the coagulation choice had a significant effect on fiber microstructure. Figure 5 shows a concentrated 5:1 weight ratio LSZ:SWNT fiber that was coagulated using 1-butanol. The image on the left shows overall macroscopic structure, while the image on the right shows microscale alignment of SWNT within the fiber. Investigations on increasing alignment and uniformity through optimizing the dispersion and coagulant chemistry and fiber spinning conditions is ongoing. Similarly, Figure 6 shows a concentrated 5:1 weight ratio LSZ:SWNT film dried on polystyrene. The electron micrograph on the left shows overall macroscopic structure, while the electron micrograph on the right shows microscale alignment of SWNT within the fiber.

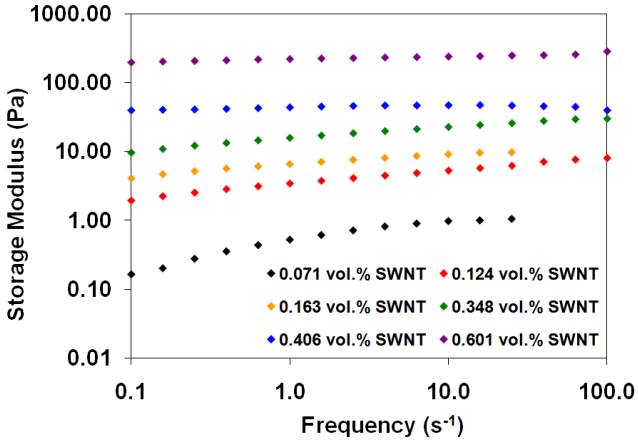

Figure 4. Frequency sweep of storage modulus as a function of angular frequency for increasing concentrations of LSZ-SWNT mixture dispersion tested at 10°C on 25 mm cone-and-plate fixture.

LSZ:SWNT Weight Ratio	Isotropic Liquid	Gel
	tan(δ)	tan(δ)
10.0:1.0	0.464	0.193
7.5:1.0	0.424	0.226
5.0:1.0	0.659	0.298
2.5:1.0	0.650	0.184

Table 1. Rheological parameter tan(δ) given immediately before and after phase transition of LSZ-SWNT mixture dispersions.

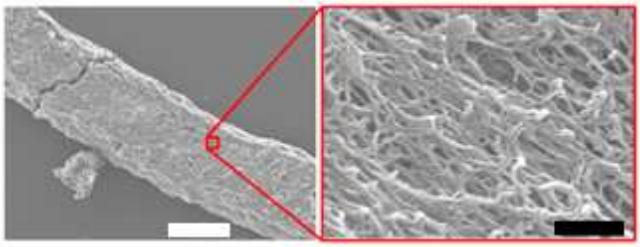

Figure 5. Electron micrographs of solution spun LSZ-SWNT fiber. Scale bars: (left) 500 μm and (right) 500 nm.

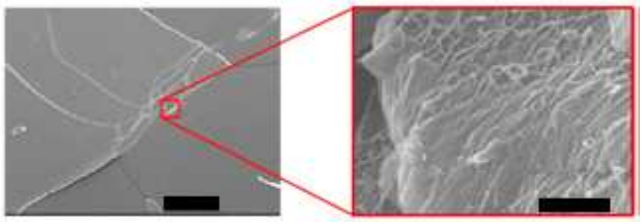

Figure 6. Electron micrographs of rotary drop-dried LSZ-SWNT film. Scale bars: (left) 1 mm and (right) 300 nm.

4 ANTIBACTERIAL ACTIVITY

Turbidimetric analysis was performed on LSZ and LSZ-SWNT samples by measuring the change in absorbance at 450 nm in an 0.015 vol.% concentration *Micrococcus lysodeikticus* solution. Figure 7 shows the change in absorbance at 450 nm of light for all four samples and a bacterial reference. The decrease in absorbance shows that the bacteria are lysed, which confirms the ability to produce LSZ-SWNT dispersions and macroscopic assemblies which maintain the antibacterial activity of native LSZ. The increased antibacterial activity of LSZ-SWNT supernatant dispersion could be due to the increased order of LSZ coupled with SWNT, which is shown by circular dichroism. However, the LSZ-SWNT mixture dispersion shows a similar secondary structure but does not show the increase in antibacterial activity. Further testing needs to be completed for confirmation of increased activity of LSZ-SWNT supernatant dispersions.

5 CONCLUSIONS

The controlled macroscopic assembly of LSZ-SWNT into films and fibers requires understanding the factors affecting dispersion microstructure and phase behavior. Both the initial dispersions and the resulting solid assemblies retain LSZ's antibacterial activity. Concentrating LSZ-SWNT mixtures results in the formation of a gel, believed to be due to LSZ interactions, and SWNT aggregates. The aggregates hinder the potential for uniform assembly. Concentrating LSZ-SWNT supernatant

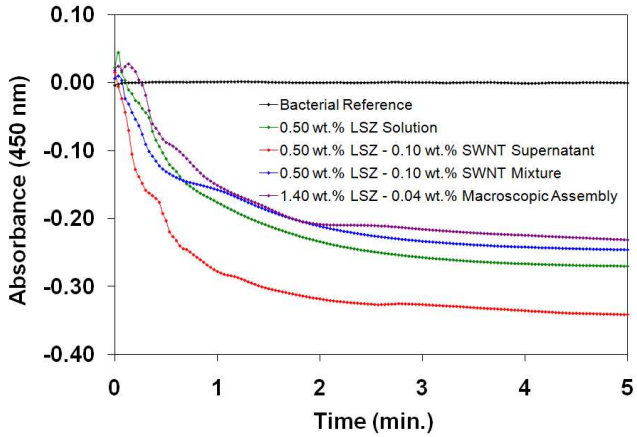

Figure 7. Turbidimetric analysis showing the change in absorbance at 450 nm of light for LSZ-SWNT dispersions and macroscopic assemblies as well as a bacterial reference.

does not result in aggregation or obvious changes in phase behavior, but is more tedious due to the lower initial concentration. Future investigations will focus on understanding the factors that affect phase behavior and the relationship between dispersion microstructure and the properties of the resulting films and fibers.

REFERENCES

1. Solvay Pharmaceuticals. Press Release, 2006.
2. Nepal, D., et al. Nano Letters, 2008, 8, 1896 – 1901
3. Krishnan, A., et al. Physical Review B, 1998, 58, 14013.
4. Walters, D. A., et al. Applied Physics Letters, 1999, 74, 3803 – 3805.
5. Hone, J., et al. Applied Physics Letters, 2000, 77, 666 – 668.
6. Nepal, D. et al. Small, 2006, 3, 406 – 412.
7. Thess, A., et al. Science, 1996, 273, 483 – 487
8. Knubovets, T., et al. Biochemistry, 1999, 96, 1262 – 1267